J. Plasma Fusion Res. SERIES, Vol. 9 (2010)

# Optimization Input Power to Obtain the Stable Annealing Conditions of a Plasma Annealing System at Atmospheric Pressure

N. Dam TRAN, Toru SASAKI, Takashi KIKUCHI, Nob. HARADA

*Plasma Laboratory, Department of Electrical Engineering, Nagaoka University of Technology*

*1603-1 Kamitomioka Nagaoka, Niigata, 940-2188, Japan*

(Received: 30 October 2009 / Accepted: 2 June 2010)

We investigated one-step, rapidly cleaning, and annealing thin wire copper using plasma generated by Dielectric-Barrier Discharge (DBD) at atmospheric pressure in a coaxial cylindrical reactor. The thin copper wire cleaning and annealing processes strongly depend on the input power, the dimensions of the reactor, and the annealing duration. The minimum input power was calculated under stable annealing conditions. When obtaining the conditions, an equivalent RLC circuit model was obtained by analyzing the sheath dynamics and power loss to the ions, electrons, and heating dielectrics during high frequency, high voltage in helium. In addition, the plasma parameters and the power balance in this system were considered. To demonstrate the optimal absorbed power for the plasma annealing system for the analysis model, comparisons of absorbed power, surface temperature of copper wire, and RMS current and voltage between the analysis model and experiments were investigated. For optimal problems, minimal absorbed power is an objective function. The design parameters were electrical efficiencies (voltage, current, frequency, and a power factor), the dimensions of reactor (the diameter of the thin wire, the discharge gap, and the discharge length), and the duration of the annealing. The inequality constraint was the breakdown discharge conditions. The equality constraints were a stable temperature for the annealing and rapid annealing conditions. The optimization results at the smallest absorbed power showed that the 0.2 mm diameter copper wire was annealed at a 20% elongation rate in the plasma reactor at an annealing velocity of 0.714 m/s.

Keywords: Annealing index, Dielectric-Barrier Discharge (DBD), optimal problem, equivalent circuit, sheath dynamic.

## 1. Introduction

The atmospheric-pressure plasma generated by Dielectric-Barrier Discharge (DBD) is widely applied in manufacturing such as ozone production, cleaning, surface modification, deposition and sterilization [1-5]. In our previous study, the cylindrical DBD plasma in helium gas was applied for rapidly cleaning and annealing thin copper wire [6, 7]. As it functions, a bombardment of ions on the wire surface, collisions between electrons and neutral particles, and sheath dynamics rapidly heat, clean, pickle, deoxidize, and polish the wire surface. The cleaning and annealing processes strongly depend on the input power and the dimensions of both the reactor and the dielectric. In this paper, we found the minimum input power of this annealing system to satisfy a rapid annealing condition.

The plasma discharges in a cylindrical DBD with length $l$, inner radius $r_1$, outer radius $r_2$, a discharge effective cross sectional area $A_{eff}$, and an effective diameter $d_{eff}$ of plasma bulk are

$$A_{eff} = 2\pi(r_2^2 - r_1^2) + 2\pi l(r_2 + r_1), \qquad (1)$$

$$d_{eff} = \frac{\pi(r_2^2 - r_1^2)l}{A_{eff}}. \qquad (2)$$

To analyze the power loss to the ions and electrons in the reactor, we must calculate the minimal input power by using the minimal conditions at each element, shown in Section 4.1. To meet the annealing conditions, the source heating from the plasma discharge must be equal to the sink heating due to conduction to the copper wire and the outside environment. This equal constraint is shown in Section 4.2. The annealing index represents the rapid annealing condition, one of the important conditions of thin wire annealing. It is a constant, represented for each property material, which performs at different temperatures and times but achieves the same elongation. Section 4.3 shows how to choose the temperature and time of annealing, with Section 4.4 showing the breakdown discharge condition, and that the magnitude of the input voltage is greater than the breakdown discharge voltage during annealing. Comparison with experiments confirms the results of the optimal calculations and this is shown in Sections 3.2 and 6.

*Author's e-mail: tndam@stn.nagaokaut.ac.jp*

## 2. Experiment setup

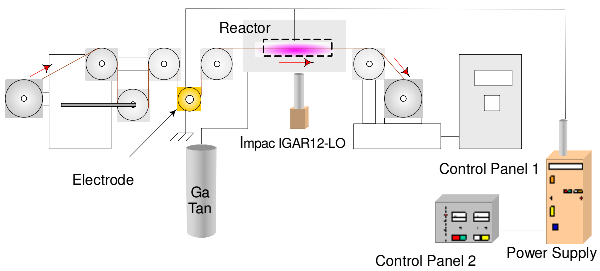


Fig. 1 Experimental setup for plasma wire annealing.

We propose an experiment where the annealing and cleaning processes can be simultaneously operated by using discharge plasma with a coaxial cylindrical DBD reactor in atmospheric pressure. Fig. 1 shows a schematic of the annealing system. The system was composed of a gas tank, a carrier with control panel 1, a power supply with control panel 2, a plasma reactor, and Impac IGAR12-LO equipment for measuring the surface temperature of the copper wire in the reactor. The gas tank is used to supply helium with reconstituted air (purity > 99.9%). The gas is fed into reactor under a controlled flow rate. The air was purged before plasma treatment. Control panel 2 controlled the voltage and the frequency. The reactor is constructed by a cylindrical dielectric inside a thin cylindrical aluminum electrode as shown in Fig. 2. The outer electrode, connected to a high power, is wrapped around the dielectric. The inner electrode, connected to the ground, is a copper wire, carried in the centre of reactor by a carrier.

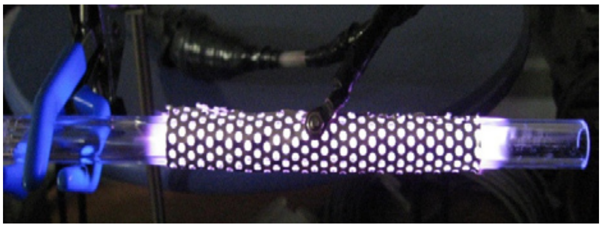

Fig. 2 The cylindrical DBD reactor.

## 3. Model analysis

### 3.1. Equivalent circuit model

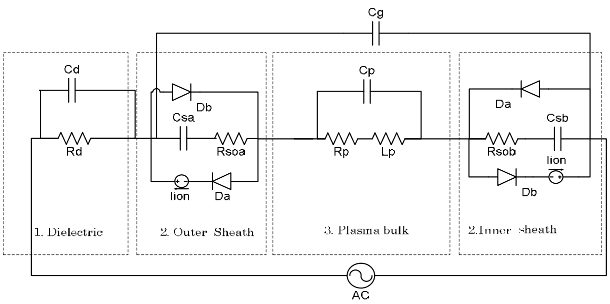


Fig. 3 Equivalent circuit model.

The circuit model reflects the physical structure of the cylindrical DBD reactor. The combination between series and parallel circuit models is equivalent to the total reactor impedance. During the first half cycle of the applied high voltage, the thin copper wire is the cathode, the electrons are driven away, and the ions are accelerated into the cathode. Electrons move faster than ions, leaving the ions behind to form an ion sheath layer near the copper wire. The sheath edge is extended to the centre by extracting new ions from the plasma. The same situation occurs in the second half cycle, where the ion sheath layer is formed near the dielectric. The plasma bulk is formed between the sheaths. A RLC electrical circuit models the plasma bulk, sheaths, and dielectric. Fig. 3 shows three main parts of the corresponding physical discharge configuration: (1) dielectric wall, (2) dynamic sheaths and (3) plasma bulk.

When the sheath fully expands on one side and shrinks on the other side, the current at the expanded side is the displacement current and the current at the shrank side is the conduction current. Here we assume that the thickness of each sheath is the Child-Langmuir sheath model [8, 9]. In sheath dynamics, the power dissipation of the oscillation sheath heating is connected to oscillation resistances, $Rso_{a,b}$ (a and b are the indices for the positions near the copper wire and dielectric, respectively). The sheath layers are connected to the sheath capacitances, $Cs_{a,b}$. The ion current in sheath, $I_i$ is parallel to the electron current, $I_e$. At the dielectric, the admittance of the dielectric is connected to the parallel of the dielectric capacitance, $C_d$ and the dielectric heating resistivity, $R_d$. At the bulk plasma, the admittance of the bulk plasma is connected to the parallel combination of the series, $L_p$ and $R_p$, with cylindrical space capacitance, $C_p$. The diodes, $D_a$ and $D_b$, are used to specify the sign of the input voltage. The gas capacitance of the reactor before discharging is also connected to the parallel $C_g$. The expressions for equivalent electrical elements are shown as follows.

For long time scale and high plasma density, the dynamic sheath radius, $r_s$ and ion current, $I_i$ flowing between two electrodes are obtained [10] by

$$\frac{dr_s}{dt} = \frac{4}{9en_e}\varepsilon_0\sqrt{\frac{2e}{M}}\frac{V(t)^{3/2}}{r_t r_s \beta^2}, \quad (3)$$

$$I_i = \frac{8\pi}{9}\varepsilon_0\sqrt{\frac{2e}{M}}\frac{V(t)^{3/2} l}{r_t \beta^2}, \quad (4)$$

where $V(t)$ is the applied voltage, $n_e$ is the electron number density, $\varepsilon_0$ is the free-space permittivity, $M$ is the ion mass, $r_s$ and $r_t$ are the sheath and electrode radius, respectively, and $\beta$ is the tabulated function of time-varying ratio, $r_s/r_t$ expressed by the infinite series

$$\beta = \mu - \frac{2\mu^2}{5} + \frac{11\mu^3}{120} - \frac{47\mu^4}{3300} + \ldots, \quad (5)$$

where $\mu = ln\,(r_s/r_t)$.

Assuming that all the ions in the sheath are implanted to the cathode surface and that the cathode is heated to the annealing temperature, the ion heating power is then

$$P_i = V(t) I_i\,. \quad (6)$$

From the dynamic sheath thickness, $S = r_s - r_t$ we can assume that the sheath capacitance in atmospheric pressure is

$$C_s = 1.52x2\pi\varepsilon_0 \frac{1}{\ln\left((r_t + S)/r_t\right)}. \quad (7)$$

Under high frequency voltage, the sheath stretches and shrinks near an electrode with a high frequency. The oscillating sheath randomly heats the electron with stochastic power, $P_{so}$ [11]. The equivalent oscillating sheath resistance is

$$R_{so} = \frac{mv_e}{2e^2 n_e}\frac{S}{A_{eff}}, \quad (8)$$

where $v_e = (8eT_e/\pi m)^{1/2}$ is the mean electron speed, $m$ is the electron mass, and $T_e$ is the electron temperature.

When plasma is generated, the characteristics of the plasma bulk are same as a resistor with plasma resistivity. The ohmic heating power, $P_{ohm}$ [11] leading to the equivalent ohmic heating resistivity is

$$R_{ohm} = \frac{m v_m d_{eff}}{2ne^2 A_{eff}}, \quad (9)$$

where $v_m$ is the electron-neutral collision frequency.

The admittance of bulk plasma leads to an equivalent RLC. This admittance is the parallel combination of the series, $L_p$ and $R_p$, with the cylindrical space capacitance, $C_p$ [11],

$$R_p = v_m L_p, \quad (10)$$

$$L_p = \frac{1}{w_{pe}^2 C_0}, \quad (11)$$

$$C_p = C_0 = 2\pi\varepsilon_0 \frac{l}{\ln(r_2/r_1)}, \quad (12)$$

where $w_{pe} = (e^2 n_e/\varepsilon_0 m)^{1/2}$ is the electron plasma frequency.

The capacitance of the cylindrical geometry dielectric, $C_d$ is

$$C_d = 2\pi\varepsilon_0 k_d \frac{l}{\ln(r_b/r_a)}, \quad (13)$$

where $r_a$ and $r_b$ are the inner and outer radius of the dielectric, respectively, and $k_d$ is the dielectric material constant.

Power lost due to dielectric heating, $P_d$ [12] is connected to the equivalent dielectric heating, $R_d$. This resistance is in parallel with the dielectric capacitance

$$R_d = \frac{d\varepsilon_r\varepsilon_0 \tan\delta}{2\pi f A}, \quad (14)$$

where $A$ is the dielectric area, $d$ is the dielectric thickness, $tan\delta$ is the loss tangent, and $\varepsilon_r$ is the relative permittivity of the dielectric material.

The capacitance of the coaxial reactor, $C_g$ before discharge is simplified to the capacitance of a cylindrical geometry

$$C_g = 2\pi\varepsilon_0 k_g \frac{l}{\ln(r_2/r_1)}, \quad (15)$$

where $k_g$ is the dielectric gas constant, and $r_1$ and $r_2$ are the inner and outer radius of the reactor, respectively.

From the equivalent circuit shown in Fig. 3, the complex impedance of the discharge is $Z = R + jX$. The absorbed power is $P_{abs} = RI_{rms}^2$, and the plasma parameters ($v_m$, $T_e$ and $n_e$) are obtained from the following three equations

$$R = \frac{V_{rms}}{I_{rms}}\cos(\theta), \quad (16)$$

$$X = \frac{V_{rms}}{I_{rms}}\sin(\theta), \quad (17)$$

$$P_{abs} = \frac{1}{\tau}\int_0^\tau V(t)I(t)dt, \quad (18)$$

where $V(t)$ and $I(t)$ are the voltage and current waveforms obtained from an oscilloscope. The V-I phase difference $\cos(\theta)$ and the apparent power in the plasma are

$$\cos(\theta) = \frac{P_{ave}}{P_{apparent}}, \quad (19)$$

$$P_{apparent} = V_{rms}I_{rms} = \left(\frac{1}{\tau}\int_0^\tau V(t)^2 dt\right)^{1/2}\left(\frac{1}{\tau}\int_0^\tau I(t)^2 dt\right)^{1/2}. \quad (20)$$

### 3.2. Comparison of numerical with experimental results

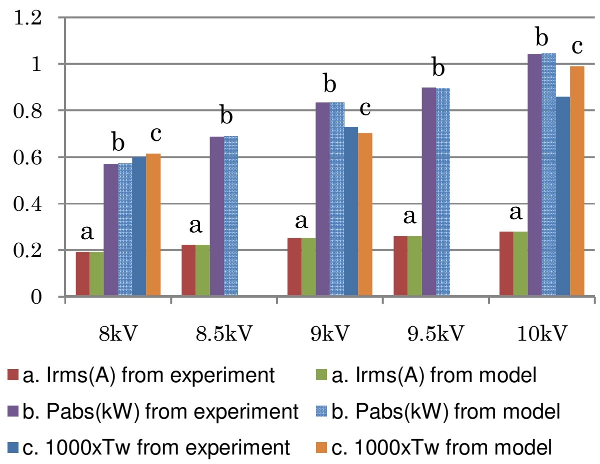


Fig. 4 Comparisons of absorbed power, surface temperature of copper wire, RMS current and RMS voltage between the analysis model and the experiment.

The plasma annealing reactor shown in Fig. 2 is modeled as an equivalent circuit shown in Fig. 3. For comparison of numerical calculations with experiment results, the geometry of the reactor is constructed by using a cylindrical dielectric inside a thin cylindrical aluminum electrode. The outer electrode (15 mm in-diameter, 0.25 mm thick, and 60 mm long wrapped around the dielectric) is connected to the high power (20[kV p-p], 2[A p-p] and 45[kHz]). The dielectric barrier discharge is a quartz tube (10 mm in-diameter, 2.5 mm thickness, and 300 mm long). The inner electrode is thin copper wire of diameter 0.2 mm, connected to the ground, and moved into the centre of reactor by carrier. The used gas is helium. The flow rate of gases was fixed to 5 l/min. The voltage and current ($V(t)$, $I(t)$) are measured in real time by an oscilloscope. Impac IGAR12-LO equipment is used to measure the surface temperature of the copper wire in the reactor. We use the input RMS voltage, $V_{rms}$ as a parameter to compare the absorbed power, $P_{abs}$, the RMS current, $I_{rms}$ and the wire surface temperature, $T_w$ between the analysis model and the experiments. The wire surface temperature is calculated by the balance power in the reactor as shown in Eq. 26.

Figure 4 shows the results of power loss, surface temperature of copper wire, and RMS current and voltage between the analysis model and the experiments. The results indicate that the absorbed power and surface temperature of the copper wire from the experiments and the analysis model are similar. We can conclude that the analysis model is acceptable for the optimal problem.

## 4. Optimal analyses

### 4.1. Minimum input power analysis

The losses due to internal power loss, Bremsstrahlung, and atomic line radiation are negligible because of the very small power comparisons with the absorbed power. The time-averaged absorbed power, $P_{abs}$, by both electrons and ions must be equal to the average dissipated power. The power dissipation to the ions is $P_{si}$. The total power dissipation to the electrons is a nonlinear sheath oscillating power at the inner and outer electrodes ($P_{soa}$, $P_{sob}$), ohmic heating power ($P_{ohm}$), and dielectric heating power ($P_d$). In this paper, the dielectric heating power was ignored because proper choosing of a dielectric material can minimize it [12]. The absorbed power, $P_{abs}$ is calculated using the following equation [11],

$$P_{abs} = \mathrm{Min}\left(\frac{m\nu_m d_{eff}}{2n_e e^2 A_{eff}} + \frac{3u_B}{2\varepsilon_0\omega^2 A_{eff}} + \frac{1mv_e}{2e^2 n_e}\frac{1}{A_{in}} + \frac{1mv_e}{2e^2 n_e}\frac{1}{A_{out}}\right) I^2, \quad (21)$$

where $u_B = (eT_e/M)^{1/2}$ is the Bohm velocity of ions, $\omega = 2\pi f$ is the angular frequency, $f$ is frequency of the applied voltage, and $A_{in}$ and $A_{out}$ are the cross sectional areas of the sheaths.

### 4.2. Power balance for annealing

The source and sink heating are the balance of the annealing temperature of the copper wire and must be equal. The source heating is generated by ions bombarding the surface. The sink heating conducts to both the copper wire and the environment. In one cycle input voltage, the ions bombard the surface of copper wire in only half the cycle. In this half cycle, the plasma discharge only happens when the input voltage is greater than the breakdown voltage, $V_b$. Assume that all ions in the sheath implanted into the copper surface create the ion source heating, described by

$$\mathrm{Pi} = \frac{1}{2}V(t)\mathrm{Ii} = \frac{1}{2}V(t)\frac{8\pi}{9}\varepsilon_0\sqrt{\frac{2e}{M}}\frac{V(t)^{3/2}l}{r_t\beta^2}, \quad (22)$$

when $V(t) \geq V_b$.

The power loss to the copper wire during annealing time $\Delta t$, annealing volume, $\Delta V$, and increasing temperature, $\Delta T_w$ in the wire is described by

$$P_{ann}\Delta t = \rho C_v \Delta V \Delta T_w, \quad (23)$$

where $C_v$ is the specific heat capacity, $\rho$ is the density, and $T_w$ is the temperature of wire surface. The power loss to the copper wire is rewritten as

$$P_{ann} = \rho C_v 2\Pi v r_t^2 \Delta T_w, \quad (24)$$

where v is velocity of copper wire.

The power dissipated by conduction to air at an ambient temperature is calculated by measuring the temperature difference between the copper wire and the outside electrode $T_{out}$[13]

$$P_{con} = \frac{T_w - T_{out}}{\frac{1}{4\pi\lambda x(3)}\ln\left(\frac{r_2}{r_1}\right)}. \quad (25)$$

The balance power in the reactor is

$$\mathrm{Pi} = P_{ann} + P_{con}. \quad (26)$$

### 4.3. Rapid annealing condition

The purpose of annealing is to use temperature to overcome the activation energy, $Q$ of the thin wire after cold working. The annealing process, which was performed at different temperatures and durations but achieved the same result, is called the annealing index I [14], and is calculated by

$$I = \frac{1}{2.303}\ln\int_0^t e^{-Q/RT_w}\,dt, \quad (27)$$

where $Q$ is the activation energy for recrystallization, $R$ is the universal gas constant, $t$ is annealing duration and $T_w$ is the annealing temperature. Depending on material recrystallization or physical properties, the annealing index can be related. Associated with the specific degree of cold working, the activation energy for recystallization can be related to

$$I = \log_{10}(t) - \frac{Q}{2.303RT_w}. \quad (28)$$

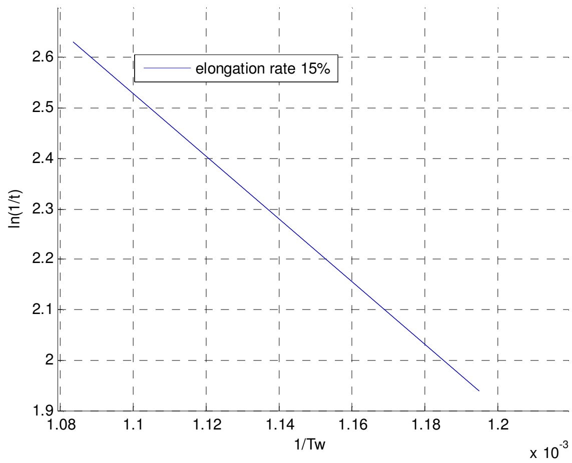


Fig. 5 A plot of $1/T_w$ versus ln(1/t)

From experiments, the activation energy ($Q$ = 5.17x$10^4$ kcal/mol) of material recrystallization associated with the cold working condition of the copper wire can be obtained by plotting data as $1/T_w$ versus $ln(1/t)$ for an elongation rate of 15% in helium. The copper wire is carried through the plasma reactor with velocities of 25 m/min and 50 m/min and temperatures of 923 K and 827 K, respectively. Fig. 5 shows the slope of a linear regression through the above data. The index annealing of the copper wire annealing at temperature 600°C and duration 0.144 s is $I$ = -4. From equation (28), two parameters ($t, T_w$) are considered, and $I$ and $Q$ are constant.

### 4.4. Breakdown discharge conditions

Experiments verified the breakdown voltage of the reactor ($V_b$) and this voltage is called the Paschen curves. This voltage depends on the pressure, the discharge gap, the dimensions of reactor, the gas type and the secondary electron emission coefficient, $\gamma$. The discharge condition is that the input voltage must be greater than the breakdown voltage

$$x(5) \geq V_b = \frac{Bpd_{eff}\ln\left(\frac{r_2}{r_1}\right)}{\ln\left(Apd_{eff}\ln\left(\frac{r_2}{r_1}\right)\right) - \ln[\ln(1+\gamma^{-1})]}, \qquad (29)$$

where $A$ and $B$ are determined by experiment [14]. For helium, $A$ = 3[1/cmTorr], $B$ = 34[V/cmTorr], and $\gamma$ = 0.3.

### 4.5. Mathematical optimal equation

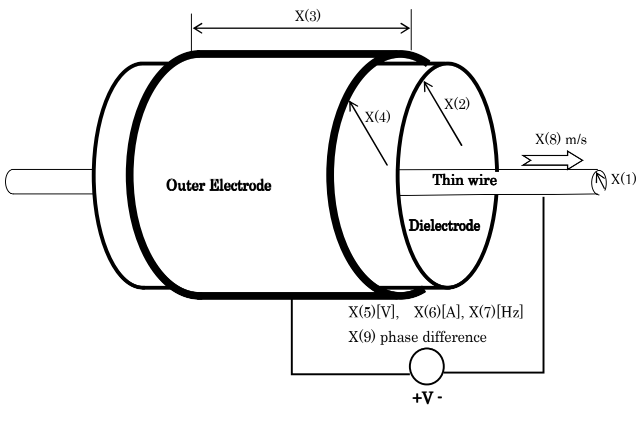


Fig. 6 Cylindrical DBD reactor with design parameters

The objective function of the mathematical optimal equations (Eq. 29) is the minimum absorbed power of the plasma reactor, shown in Fig. 6, where the design parameter, ***X(i)***, $i$ = 1-9, is shown in Table 1. The nonlinear inequality constraint is the breakdown discharge condition, and the nonlinear equality constraints are the rapid annealing condition and the heating balance annealing. The boundary inequality constraints are the discharge gap and dielectric thickness. The mathematical optimal equations are

$$\text{Min } P_{abs} = \text{Min}\left[\left(\frac{m\nu_m d_{eff}}{2n_e e^2 A_{eff}} + \frac{3u_B}{2\varepsilon_0 w^2 A_{eff}} + \frac{1mv_e}{2e^2 n_e}\frac{1}{A_{in}} + \frac{1mv_e}{2e^2 n_e}\frac{1}{A_{out}}\right)x^2(6)\right], \qquad (29)$$

with constraints

$$\begin{cases} \mathbf{X_{lb}} \leq \mathbf{X} \leq \mathbf{X_{ub}} \\ \mathbf{AX} \leq \mathbf{b} \\ \mathbf{C} \leq \mathbf{0} \\ \mathbf{C_{eq}} = \mathbf{0} \end{cases}, \qquad (30)$$

where

$$\mathbf{A} = \begin{bmatrix} 1 & -1 & 0 & 0 & 0 & 0 & 0 & 0 & 0 \\ 0 & 1 & -1 & 0 & 0 & 0 & 0 & 0 & 0 \end{bmatrix}, \qquad (31)$$

$$\mathbf{b} = \begin{bmatrix} -0.0001 \\ -0.0001 \end{bmatrix}, \qquad (32)$$

$$\mathbf{C} = \frac{Bpd_{eff}\ln\left(\frac{x(2)}{x(1)}\right)}{\ln\left(Apd_{eff}\ln\left(\frac{x(2)}{x(1)}\right)\right) - \ln[\ln(1+\gamma^{-1})]} - x(5), \qquad (33)$$

$$\mathbf{C_{eq}} = \begin{bmatrix} P_{Ion_h} - P_{ann} - P_{con} \\ \log_{10}(t) - \frac{Q}{2.303RT} - I \end{bmatrix}, \qquad (34)$$

and the upper and lower boundary condition of **X** are,

$\mathbf{X_{lb}}$ = [0.0001;0.0005;0.01;0.007;5000;0.01;9000;0.2;0.2], (35)

$\mathbf{X_{ub}}$ = [0.0001; 0.1; 4; 0.2; 12000;5; 50000; 3; 0.9]. (36)

Table 1. The design parameters of the cylindrical DBD reactor plasma for the wire annealing.

| Parameters **X** | Description |
|---|---|
| x(1)[m] | Inside radius of reactor |
| x(2)[m] | Outside radius of reactor |
| x(3)[m] | Length of reactor |
| x(4)[m] | Outside radius of dielectric |
| x(5)[V] | RMS Input voltage |
| x(6)[A] | RMS Input current |
| x(7)[Hz] | Input frequency |
| x(8)[m/s] | Velocity of carrier |
| x(9) | Power factor |

### 5. Optimal results and discussion

The reactor is supplied by helium with a thermal conduction of 0.142 W/mK and constructed by a cylindrical quartz dielectric inside a thin cylindrical aluminum electrode. The secondary electron emission coefficient is chosen as $\gamma$ = 0.3. Based on experiment, the annealing index of the activation energy 5.17x$10^4$ kcal/mol, is -4, the universal gas constant is 8.314, and the annealing temperature, $T_w$ = 600°C. The result of the design parameters from optimal calculation are

**X** = [0.0001; 0.005; 0.0833; 0.0075; 4,540; 0.2915; 45000; 0.714; 0.6844].

and the absorbed power, $P_{abs}$ = 905 W. This result shows that to anneal a 0.2 mm diameter copper wire with a 0.417 m/s carrier speed and an elongation rate greater than 20%, we have to setup the dimensions of the reactor as follows: outside radius 5 mm; length 83 mm; outside radius dielectric 7.5 mm; RMS input voltage power supply 4,540 V; RMS input current 0.291 A; and 45,000 Hz frequency. For a plasma annealing system in reality, an impedance mismatch must prevent the reflected power from the plasma reactor back to the power supply. The power factor of the system is the data to design a parallel matching network with a plasma reactor. The carrier velocity and the length of the reactor are proportional and are parameters of the constant index annealing function. If we want to increase outcome product, we have to increase the length of reactor.

## 6. Comparable results and discussions

Table 2 shows the comparison between the results of the experiments and the optimal calculation at the same initial conditions, with experiment parameters: gas type He, dielectric material BN, gas flow rate 5 l/min, dielectric thickness 2.5 mm, gap length 5 mm, reactor length 60 mm and frequency 45 kHz. At the same initial conditions, we obtained the same design parameters: electrical efficiencies (voltage, current, and frequency), dimension of both reactor and dielectric, annealing duration, and power loss. Again, we can conclude that the analysis model is useful for the optimal analysis.

Table 2. The result of design parameters from optimal calculation and from experiment.

| Parameters **X** | Experiment | Optimal calculation |
|---|---|---|
| Gas | He | He |
| x(1)[m] | 0.0001 | 0.0001 |
| x(2)[m] | 0.005 | 0.005 |
| x(3)[m] | 0.06 | 0.05 |
| x(4)[m] | 0.0075 | 0.0075 |
| x(5)[V] | 5540 | 5540 |
| x(6)[A] | 0.278 | 0.26 |
| x(7)[Hz] | 45000 | 45000 |
| x(8)[m/s] | 0.416 | 0.416 |
| x(9) | 0.679 | 0.679 |
| $P_{abs}$[Watt] | 1006 | 1000 |

## 7. Conclusions

In summary, the characteristics of annealing by cylindrical DBD were investigated by analyzing the sheath dynamics and the power loss to ions and electrons during high frequency and high voltage in helium. A RLC equivalent circuit modeled the physical structure of the cylindrical DBD. The annealing temperature generated by the ion heating power in the analysis model is similar to the one measured from the experiments, which demonstrates that the analysis model represents an annealing reactor. From the optimal calculations, the dimensions of the coaxial cylindrical DBD plasma were recalculated to meet the discharge conditions. The velocity of the copper wire in reactor was also calculated to satisfy the rapid annealing condition. The most important finding of this study is that with minimum input power, the annealing conditions of the present plasma annealing system at atmospheric pressure can still be guaranteed.

## 8. References


[1] Ulrich Kogelschatz, Plasma Chem. Plasma Process. **23**, 1 (2003).

[2] Yu.V. Filippov and Yu.M. Emelýanov, Russ. J. Phys. Chem. , **32-12**, 2817 (1958).

[3] J.Y. Jeong, S.E. Babayan, V.J. Tu, J. Park, I. Henins, R.F. Hicks and G.S. Selwyn, Plasma Sources Sci. Technol. **7,** 282 (1998).

[4] S.E. Babayan, J.Y. Jeong, V.J. Tu, J. Park, G.S. Selwyn and R.F. Hicks, Plasma Sources Sci. Technol. 7, 286 (1998).

[5] M. Koide, T. Horiuchi, T. Inushima, B.J. Lee, M. Tobayama and H. Koinuma, Thin Solid Films. **316,** 65 (1998).

[6] T. Nakamura, Ch. Buttapeng, S. Furuya, N. Harada: 2nd IEEE international conference on power and energy (PECon 08) December 1-3, 2008, Johor Baharu, Malaysia.

[7] T. Nakamura, Ch. Buttapeng, S. Furuya, N. Harada: VASSCAA-4. **256-4**, 1096 (2009).

[8] C. D. Child, Phys. Rev.. **32-5**, 492 (1911).

[9] I. Langmuir, Phys. Rev.. **33-6**, 954 (1929).

[10] Scheuer, J. T., Shamim, M., and Conrad, J. R., J. Appl. Phys., **67-3**: 1241 (1990).

[11] M. A. Liberman and A. J. Lichtenberg, Principles of Plasma Discharges and Materials Processing. New York: Wiley, 1994.

[12] J. Reece Roth and Xin Dai, AIAA , **1203**, 6 (2006).

[13] H. Sadat, N.Dubus et al., Applied Thermal Engineering, **29**, 1259 (2009).

[14] F.F.Kraft, R.N. Wright, and M.K. Jensen, JMEPEG, **5**, 213 (1996).